Design of a low pressure turbine stage with control stage characteristics for investigations of partial admission effects

Omer Hodzic, Martin Sinkwitz, Andreas Schramm, Senad Iseni, David Engelmann, Francesca Di Mare, Ronald Mailach

Design of a low pressure turbine stage with control stage characteristics for investigations of partial admission effects

Omer Hodzic[1], Martin Sinkwitz[1] Andreas Schramm[1], Senad Iseni[1], David Engelmann [1], Francesca di Mare[1], Ronald Mailach[2]

ISROMAC 2017

International Symposium on Transport Phenomena and Dynamics of Rotating Machinery

Hawaii, Maui

December 16-21, 2017

Abstract

Partial admission is commonly used to control the power, especially of small scale steam turbines. However, asymmetric flow field results at the inlet of a turbine stage with part load control when one or more nozzles are closed. In this case a highly transient flow field with specific partial admission effects occurs. Especially the control stage of the turbine is high loaded in case of partial admission and therefore, additional losses result in the flow field. Those effects are investigated insufficiently, especially experimental data are rare. In this paper the reconstruction of an existing low pressure test facility to a control stage will be presented at first. According to the new stage design three dimensional CFD calculations are carried out with focus on the estimation of unsteady fluctuations and field of influence due to partial admission. Also the positions, where the important effects are noticeable are determined. After the numerical based design process and the numerical investigation to partial admission the test facility was modificated and the measurement positions in the test facility are established.

Keywords

Partial Admission — Numerical based design process — turbine facility — control stage

[1] *Chair of Thermal Turbomachines, Ruhr-Universität Bochum, Bochum, Germany*

[2] *Chair of Turbomachines and Flight Propulsion, Technische Universität Dresden, Dresden, Germany*

INTRODUCTION

Due to the decentralization of energy supply in the future, small scaled steam turbines will be more often used. Further, common and promt load change must be ensured and the power output must be adapted to fit the needs of the consumers. For this an appropriate method to control the power output have to be chosen considering efficiency, economy and ecology. Partial Admission is in terms of efficiency at part load operation points an effective method to control the power output of small scale steam turbines. In this case upstream of the turbine a so called control stage is applied. The load of the stage is controlled by a group of nozzles, each with control valves, which are located in circumferential direction. At part load operation one or more nozzle groups can be partially or completely closed resulting in a asymmetric flow distribution in circumferential direction. As a result the static pressure and static enthalpy drop are increased over the control stage and simultaneously reduced downstream of the control stage.
Additionaly flow losses and an increasing stage load, especially on the rotor blades, occur. The mixing effects at the boundary between the admitted and non admitted annulus arc lead to specific losses at partial admission. Furthermore, pump effects in the rotor passages downstream of the non admitted area as well as filling and emptying of rotor passages that pass the non admitted area cause additional losses.
Several research investigations of partial admission effects are described in literature. Most of these investigations are numerical studies whereas experimental investigations are rare. Hushmandi [7] and Kalkkuhl [9] present detailed numerical simulation results. Fridh et al. [4] and references [3], [15], [2] presents experimental results to partial admission effects. The mentioned experimental investigations comprise mainly traverses in different planes of the control stage and the turbine. In the work of Fridh unsteady loading of a rotor blade due to the part load is investigated with time resolved pressure transducers and strain gauges. Although numerical investigations ([5] [10] [6] [14][13]) are given in detail, experimental data are necessary to validate the numerical models.
In order to understand effects resulting from part loading more experimental investigations to partial admission effects are essential.
At the Chair of Thermal Turbomachinery, Ruhr-Universität Bochum a large scale low pressure test facility is proposed to used for the above mentioned experimental investigations. To achieve comparable flow conditions between the test rig and a control stage of industrial turbine the test rig has to be modified. Additionally, the characteristics of the necessary measurement technique has to be specified. The aim of this work is the design

of a suitable stage geometry with characteristics of a control stage as well as the estimation of the unsteady fluctuations at full and partial admission conditions. For this, a numerical based design process is conducted. In a first step steady state simulations are performed using a reduced numerical model with one stator and two rotor passages to reconstruct the low pressure air test stage. The reduced numerical model was investigated for a number of different blade numbers, channel heights and operating points. These investigations result in a final construction, which was used for the subsequent studies. In a next step steady state and transient simulations of a 360 degree model of the designed stage for the full admitted case (reference case) and a case with partial admission are carried out. Based on this results the time dependent fluctuations are estimated and the field of influence caused by partial admission are determined.
Subsequently, the reconstruction of the existing test facility to the new control stage design and the implementation of the measurement setup are realized. In the following two sections a description of the existing test facility and the detailed design process are discussed.

1. TEST FACILITY

An existing low pressure test facility is applied for the planned experimental investigations to partial admission effects. In the original configuration this facility includes up to two stages and is supplied with air by a radial blower positioned downstream of the stage. The test turbine operates in a suction mode. At the inlet of the test facility the air is under ambient conditions. Due to the large test rig the disturbance caused by the installed measurement equipment is negligible. The test section consists, depending on the configuration, of one or more stationary or rotating replaceable components. The benefit of this modular construction is that investigations to other unsteady effects can be carried out with moderate retrofit effort. For example, experimental investigations of the interaction of different secondary flows are carried out by Sinkwitz et al. [12]. The inlet casing includes two rectifiers to adjust the air in the axial direction. Behind the inlet casing different stage configurations can be realized. The rotor is mounted on the machine shaft which contains of a outer component and a inner component. The rotor is fixed on the outer shaft whereas measurement devices are able to implement in the inner hollow shaft.
Two pivoted casings occupy several accesses for measurement probes and allow a stepwise circumferentially move. Additionally, the probes can be traversed in radial direction. The inlet casing and the outlet casing include accesses for pressure probes or temperature measurement devices. Further, the outlet casing includes 10 evenly distributed pressure taps in circumferential direction for measuring the static pressure at the stage outlet. In combination with the total pressure at the turbine inlet the operating point can be monitored and controlled. In addition, the flow rate can be determined by measuring the difference of static pressure downstream and upstream of a channel contraction in the inlet casing.

Table 1. Test facility characteristics (before design process)

Power of blower $P_{blower}[kW]$	150
Massflow $\dot{m}$ $[kg/s]$ (at DP [1])	12.8
Shaft speed of turbine n_T $[rpm]$ (at DP)	500
Velocity at stage inlet c_0 $[m/s]$ (at DP)	15
Mach number at stage inlet Ma_0 $[-]$	≈ 0.1
Reynolds number at stage inlet Re_0 $[-]$	≈ 200000

2. CONCEPTUAL METHODS

Step 1: Design of a control stage geometry

The stator and rotor blade design as well as the stage configuration are determined by scaling an existing blade geometry used in a control stage of an industrial steam turbine and by variation of the blade numbers in the stator and rotor row simultaneously. The purpose of this blade variation was the adjustment of the dimensionless stage variables e.g. the distribution of the pressure coefficient c_p along the blade chord, degree of reaction $\rho_{y,s}$ and the stage loading Ψ_y to corresponding values of a control stage in a industrial steam turbine. The mentioned variables are defined as:

$$\rho_{y,s} = \frac{y_s''}{y_s} \qquad \Psi_y = 2\frac{y}{u_2^2}$$

For that, at first an existing blade geometry was scaled up to the channel heigth of 170mm and several combinations of the blade number ratio $\frac{z_{rotor}}{z_{stator}}$ were investigated by numerical simulations. Therefore, two numerical models, one for the industrial steam turbine under origin conditions and one for the test facility under ambient conditions are calculated and compared. For both numerical investigations a one stator and two rotor passage blade passage model are used. The SST-turbulence model is used and steady state simulations for both numerical setups are carried out. The scaling of the origin geometry results in very large dimensions so the assembly in the existing low pressure turbine is not realizable. Therefore, the channel height (origin height: 170mm) was customized and simultaneously the blade number of the stator and rotor row were noticeably increased. A raised number of blades allows, a larger number of blocking configurations. Due to a smaller pitch, more suitable degrees of blocking adjusted to a stable operating point of the blower are realizible. In contrast the test rig channel decreased and consequently, the influence by the endwalls will be raised. To avoid strong influence by the endwalls of the test facility as well as the influence by the measurement probes a channel height of 80mm was chosen.
After determination of the channel height, the operating point with the best efficiency (design point) was to be determined. Therefore, different variations of rotational speed of the rotor and of the massflow rate as well as variations of the blade number ratio $\frac{z_{rotor}}{z_{stator}}$ are carried out. Here, a stable operation

[1] DP=design point

of the blower has to be ensured. Especially at partial admission conditions caused by additional losses a large shift in the compressor map of the blower can be expected as shown in the next section.
At the same time, the stage characteristics should be comparable with corresponding values of above mentioned steam turbine control stage at midspan.
In conclusion, it is necessary to achieve similar velocity triangles in the relative frame for similar distribution of the pressure coefficient $c_{p,rel}$ as well as the reaction of degree and the stage loading. Additionally, the best efficiency will be achieved at this conditions for a given rotational speed of the rotor. The best efficiency point raises with increasing rotational speed n_T and massflow rate $\dot{m}$ as long as the velocity triangles are not changed. However, the pressure and enthalpy drop over the stage increase simultaneously. At the limit of the blower power a stable operation point can not be ensured.
The determination of the design point based on results of steady state calculations at full admission conditions. The rotational speed and the massflow were defined first and will be changed if the resulting pressure drop over the stage is to high considering the expected increasing of the pressure drop caused by flow losses at partial admission conditions. So the suitable operating point results from a iterative process.
Thus, the design point is defined at a massflow rate of $\dot{m} = 7kg/s$ and a shaft speed of $n_T = 500rpm$ with a blade number combination of 44 stator and 75 rotor blades even though better efficiency can be achieved at higher massflow.
The pressure coefficient is determined by referencing on velocity in the relative frame. So the definition of $c_{p,rel}$ is:

$$c_{p,rel} = \frac{p - \overline{p}_2}{\frac{1}{2}\overline{\rho w}_2}$$

Due to this definition, the influence by the different rotational speed in industrial steam turbines and in the presented LP turbine will be unconsidered. At that operating point the degree of reaction is $\rho_y < 0.1$ and the stage loading $\Psi_h \approx -2.92$.
Figure 1 shows the corresponding distribution of the pressure coefficient on the rotor blade at midspan for the investigated cases. A good agreement between origin and RUB control stage is recognizable except a small area at the suction side near leading edge. Based on these studies, the configuration with 44 stator and 75 rotor blades will be used for further numerical investigations. In the following, the allowed degree of blocking for the partial admission investigations has to be estimated.

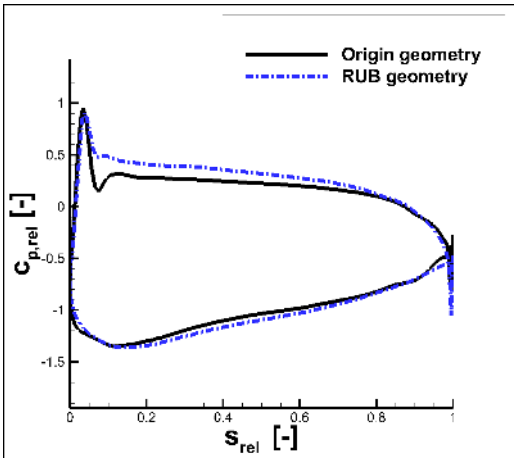

Figure 1. Pressure coefficient distribution for the origin and scaled geometry RUB

Step 2: Determination of allowed blockage ratio amount

A large number of partial admission configurations are neccesary to determine influences by the degree of blocking on magnitudes of the forces on the rotor blades. However, the arc of the blockage is limited due to design and air supply constraints. The different configurations of partial admission are investigated and depicted in the compressor map of the blower. Figure 2 shows the results at full and partial admission condition respectively ($40[deg]$ or $\epsilon = 88.89\%$). Based on this studies a degree of blocking of 40 degrees is considered. However, the blocking arc was increased up to $40.90[deg]$ resulting in 5 blocked stator passages to ensure that the ends of the blocking arc end at two edges of the stator blades. Moreover, a sufficient large area near the blockage can be investigated by traversing along the blockage till approximatly ≈ 33 degrees from the blokage borders. A large shift of the pressure difference due to partial admission compared to full admission is recognizable whereby increasing of the massflow results in a increased shift. However, a stable operation under partial admission condition is ensured.

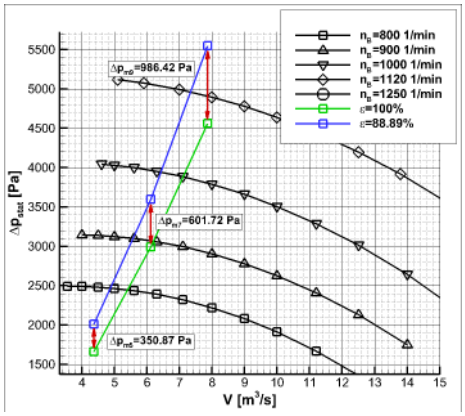

Figure 2. Air blower map

Step 3: Design adjustments of modified facility

In this section the retrofitted test facility is described and depicted. To reduce the channel height from 170mm to 80mm in the inlet casing a ramp is constructed based on CFD preinvestigations. The rotor and stator blades are mounted on wheels whereby the hub diameter is adjusted to achieve a channel height of 80mm. The hub ring of rotor wheel is connected with the shaft ring by 8 struts and the shaft ring is fixed on the shaft by slot and key. Different from the rotor construction, the stator casing is fixed at the facility frame and the hub is carried by the stator blades. In figure 3 the setup of the retrofitted test facility is depicted.

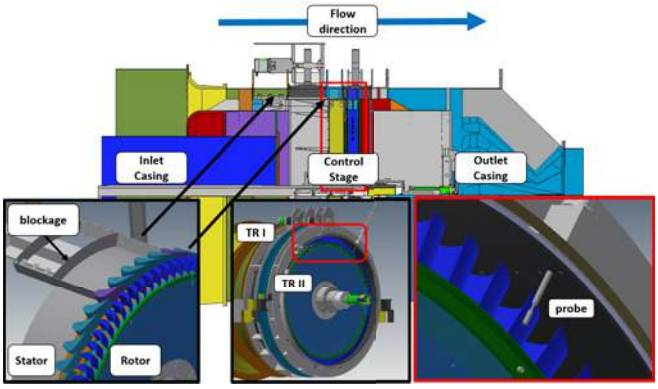

Figure 3. Retrofitted low pressure test facility

Next to the inlet casing the first pivot-mounted casing (TR I) is integrated followed by the stator casing. Behind the stator casing the rotor wheel is fixed on the shaft, whereby the axial distance between stator trailing edge and rotor leading edge amounts to $l_{ax,rotor} = 38mm$. The second pivot-mounted casing (TR II) is located coaxial above the rotor. This allows traverses between the stator and rotor row as well as traverses in three planes behind the rotor. The outlet casing is placed downstream of the stage and before the air blower. As mentioned, 10 pressure taps at the casing are used to monitoring and controlling the operating point.

Step 4: CFD and FEM calculations of the designed stage

The design process is completed by performing steady state as well as transient simulations of a 360 degrees model of the control stage. For full and partial admission case evaluation at the measurement locations are carried out to determine the influence of the perturbation areas caused by the stage geometry e.g. the blockage construction. Especially the impact of the blockage construction on the velocity and pressure field has to be captured. Furthermore, the stage load at full and partial admission conditions should be determined. Therefore, rotor blade forces will be monitored and compared for both admission cases. The results from this calculations allow specification of suitable measurement components for the experimental investigations. A detailed description of this step follows in the next section.

3. NUMERICAL INVESTIGATONS FOR PARTIAL ADMISSION

In this section numerical investigations are presented by using CFD and FEM analysis for calculation of the flow field as well as the structural behavior. The CFD investigations include steady state and transient calculations at full and partial admission conditions considering the proposed measurement campaigns. The evaluation of the results are carried out at the proposed measurement positions. Additional, structural analysis by using FEM methods are performed for different speed of rotation to capture the structural response frequencies of the system by comparing with frequencies of excitation due to flow field.
Hereafter, the intended measurement campaigns and the corresponding probe positions will be shown in detail and then the numerical setup will be presented.

Intended measurement campaigns

Evaluation of the numerical results were carried out in the corresponding measurement planes of the proposed experimental investigations. Additionally, the specification of the measurement technique will be determined based on the numerical results presented in this paper. Thus, the proposed measurement campaings will be presented in this section. The experimental investigations include three successively executed measurement campaigns. In the first campaign four planes of the stage will be investigated, whereby time averaged data will be measured by a five hole probe and time resolved data will be measured by two different hot wire probes. Figure 4 shows the measurement planes.

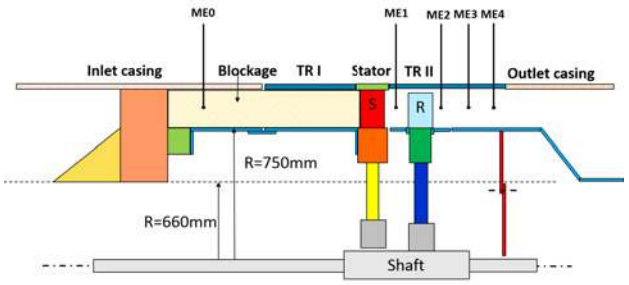

Figure 4. Measurement planes

The hot wire probes of type 55R56 will be used for measuring axial and radial velocity components and the type 55R57 for measuring axial and circumferential components. Traverses in spanwise and circumferential direction in the investigation planes ME1 as well as ME2-ME4 are intended. In these planes wall pressure will be measured by using pressure taps attached on the mentioned pivotable casings. This enables a high spacial resolution in the circumferential direction. Therefore, two different attachments will be mounted at the pivotable casing. The first one features pressure taps and the second one allows mounting of a screw-on Kulite pressure transducer. This allows aquisition of accurate time averaged as well as time resolved data at the casing of the stage.

In the second campaign pressure tabs at rotor midspan and flush mounted Kulite transducers (Kulite LQ-125) are used to measure the static pressure on the blade surface. Figure 5a and 5b shows the rotor blade with pressure tabs and the rotor blade with mounted Kulite transducers.

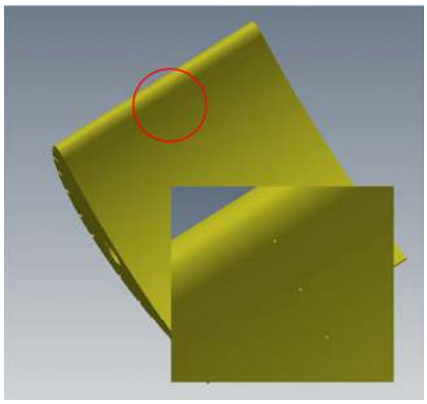

(a) Pressure tabs on pressure side of a rotor blade

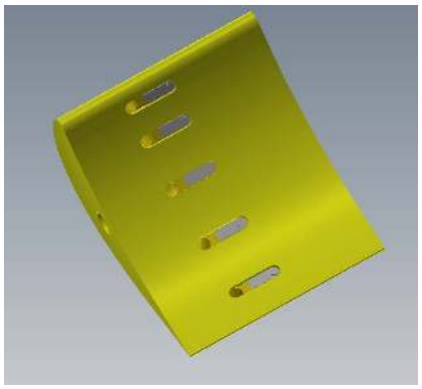

(b) Kulite transducers on pressure side of a rotor blade

Figure 5. a) Rotor blade with 12 pressure tabs on pressure side (15 tabs on suction side) b) Rotor blade with 5 Kulite transducers on pressure side (7 Kulite transducers on suction side)

The circumferetial position of the rotor can be determined by a trigger signal, which is measured for each revolution. To avoid the stochastic influences the sampling rate is defined by a measurement study with different count of sampling data. The data transfer from relative frame to the reference frame of the rotor system is realized with a slip ring system and a compact data logger system, implemented in the hollow shaft. For the time averaged pressure measurements on the rotor blade, the pressure taps are connected with a 64 channel pressure trancducer ZOC 33/64 (Scanivalve) and subsequently the analog data are transfered by the slip ring. Pressure fluctuation on the Kulite transducers are recorded as analog signals by the data logger system (Delphin ExpertVibro) and transformed to digital signal by a A-D converter. The digital data are stored on the internal hard drive and sended as one sampling for each circumferential position to the computer. Measurement of the velocity field by the Particle Image Velocimetry (PIV) method completes the experimental investigations. A concept for the PIV system is mounted on the pivot-mounted casings and allows a traverse in circumferential direction and the positioning of the system in the four different measurement planes. These concept allows the measuring of the velocity at the midspan area between the stator and rotor row, in the rotor passage and downstream of the stage.

Numerical setup

CFD analysis

In this section the numerical setup for the CFD and subsequently the setup for the FEM analysis will be described. Due to the partial admission configuration with a degree of a blockage of 40.90 degree a periodic boundary condition in circumferential direction is not possible, so the control stage have to be modeled as a full annulus model. All numerical investigations are carried out for the full admitted case (as reference) as well as for the part admitted case.

The grids of stator and rotor passages as well as the inlet and outlet domains are generated with the inhouse meshing tool AxTurboMesh [8][1]. Overall a mesh with approximately 20 million elements is used whereby the blockage are assumed as infinity thin with no slip wall conditions. In addition, all hub, shroud and blade walls assumed as no slip walls. A detailed grid independent study was conducted within a master thesis by Mutlu [11]. The results of this study show a grid independency at approximatly 20 million elements (figure 6).

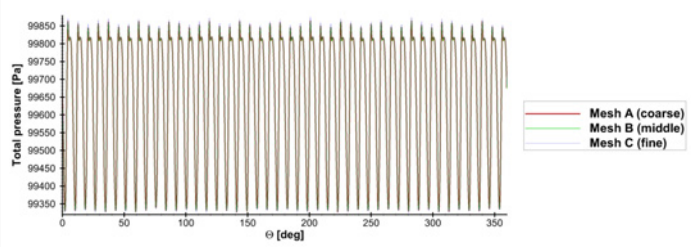

Figure 6. Grid independeny study (Total pressure in plane between stator and rotor)

The inlet domain with the stator row as well as the outlet domain are stationary whereas the rotor domain is rotating with a shaft speed of 500 rpm.

For the reference case, at inlet total pressure is set to pressure of ambient whereas at outlet boundary a massflow of $\dot{m} = 7kg/s$ is set first. Based on a steady state simulation the corresponding static pressure at outlet was determined by averaging. In the next step the averaged static pressure is defined as the outlet boundary condition. The same total pressure at inlet as well as the same static pressure at outlet were defined for the partial admission case. Thus, the pressure drop at part as well as at full loading is same. As a result, the blade forces in the admitted arc of the partial admitted configuration and of the full admitted configuration are equal. This allows a usefull comparison of forces at partial admission and full admission because all forces can be related to common reference value.

Air assumed under ideal gas conditions is used as working medium and the total temperature is set to ambient temperature of approximately $25°C$. The SST-tubulence model is used and steady state and transient simulations are carried out. Steady state simulations are performed with the so called frozen rotor interface in order to connect rotating and non rotating parts. For transient simulations a total number of 16 and 32 timesteps per blade passing of the stator blade has been chosen for a timestep study. The differences between the forces calculated with the mentioned timesteps are negligible for the partial admission and full admission case. Based on these results, further increasing of the timestep count is not necessary. Additional steady state simulations are carried out to determine the performance and efficiency of the test facility and to estimate the losses at different operating points.

FEM analysis

In addition to the CFD analysis a modal analysis was carried out to determine the eigenfrequencies of the rotor blades. The eigenfrequencies are plotted in a Campbell diagram over the rotational speed as well as the graphs of excitation frequencies (figure 13). The excitation results from stator wakes caused by trailing edges and from partial admission caused by interaction of admitted and non admitted arcs. For the modal analysis material data are used from data sheets to ensure the correct behaviour of the rotor components. Figure 7 shows the materials of the rotor components

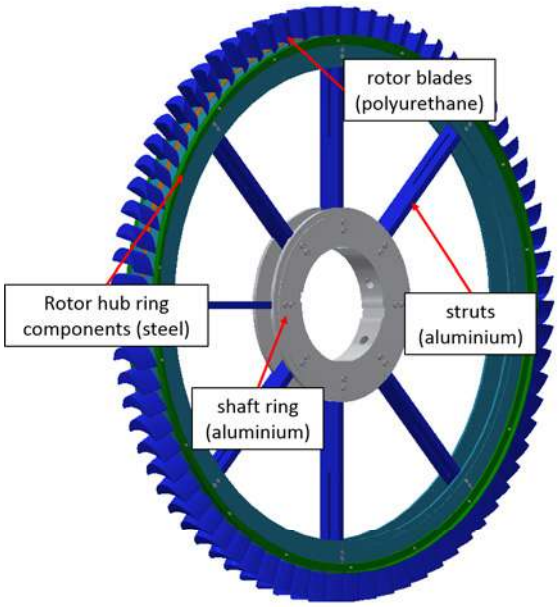

Figure 7. Material of rotor components

4. RESULTS AND DISCUSSION

In this section CFD and FEM results are presented and discussed for the full and partial admission case. Initially, results from steady state simulations will be described and evaluated. Afterwards, results from the transient calculations will be discussed, especially the time history of blade forces is explained in detail. Finally, the blade passing frequency and the frequency of disturbance caused by the partial admission will be plotted in a frequency spectra and compared with the eigenfrequencies of the rotor wheel. Further frequencies occurring in the spectra are assessed in terms of importance for the investigations, so that dominated frequencies can be captured.

4.1 Results from steady state simulations

Results from steady state calculations are presented in corresponding planes of the proposed measurement campaigns. The figures 8 and 9 show the pressure distribution in the plane ME1-ME4 for full and partial admission.

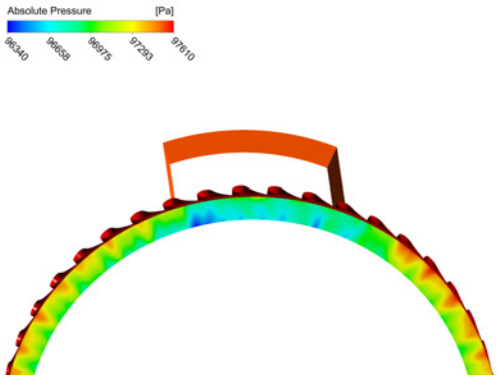

Figure 8. Absolute pressure in plane ME1 at partial admission

At the admitted arc of the stage in plane ME1 local disturbance of pressure are merely caused by blade wakes from the stator row, whereby ME2, ME3 and ME4 flow disturbance is caused by wakes of the rotor blades. All mentioned wakes generate losses and influence the efficency of the turbine directly but are relatively low compared with losses caused by part loading. Although in plane ME1 the field of influcence by partial admission is limited mainly to the arc of blockage, transporting of losses by the rotor in circumferential direction are noticeably. Therefore, it can be considered that losses are transported in circumferential direction in the ME2, ME3 and ME4 planes. A remarkable disturbance due to the part loaded stage occurs up to ME4. The rotation of the rotor and the stagger angle of stator induce a momentum in circumferential direction. These effects cause an increase of the mixing intensity between the admitted and non admitted arc.
Figure 10 shows the distribution of static entropy at midspan. Far downstream of the stage the field of influence by part loading decreases noticable. The entropy production caused by the stator wakes is distinctly less than the losses caused by the specific effects results from the partial admission. It has to be mentioned that the momentum in circumferential direction causes the disturbance to propagate in direction of the rotation even though, a sufficient range can be traversed by rotation of the pivotable casings.

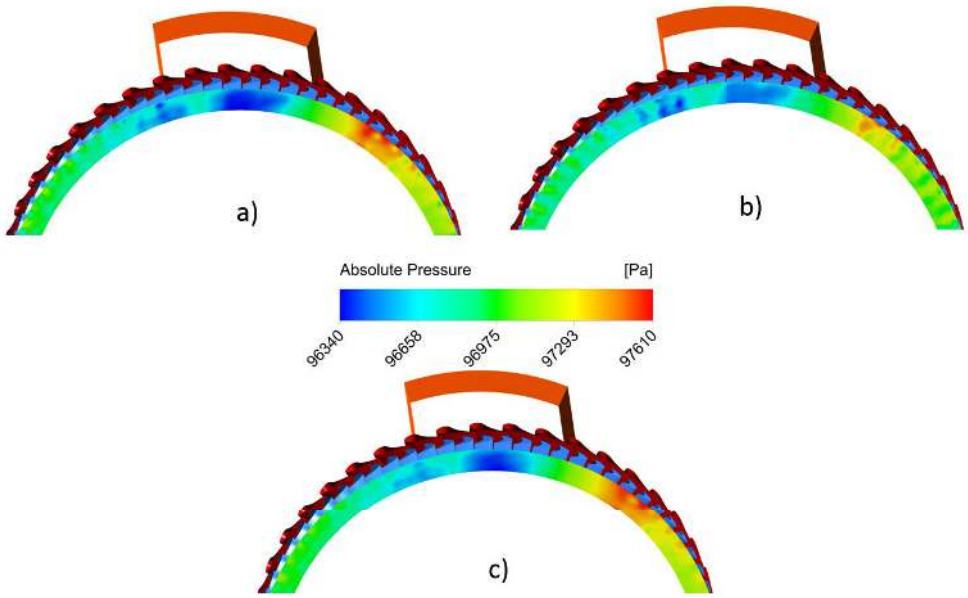

Figure 9. Absolute pressure in plane ME2, ME3 and ME4 at partial admission

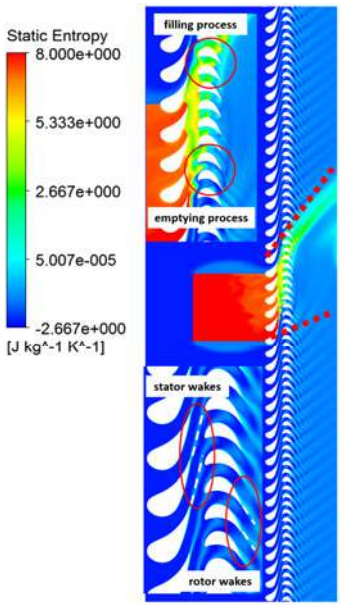

Figure 10. Static entropy under partial admission condition

4.2 Results from transient simulations

Results from steady state simulations provide time averaged data of the flow field but are not suitable to describe the highly unsteady flow field at partial admission conditions. Especially the influence by the rotation of the rotor row, the interaction between the rotor and stator blades as well as the disturbances caused by stator wakes and the blockage have to be described based on transient data. Therefore, in the following results from transient calculations of the full admitted and part admitted case are presented and compared. These investigations are carried out to determine the force response of the rotor blades due to excitation by passing through stator wakes as well as through the non-admitted section at partial admission. Furthermore, data from transient calculations allow estimation of unsteady fluctuations in the flow field and therby the specification of necessary measurement equipment can be determined.

Blade forces

At full admission conditions the wakes of the stator row cause excitation of the rotor blades. The forces are determined by the rotational speed of the rotor and the blade count in the stator row. Due to partial admission of the control stage additional excitation is caused by filling and emptying of the rotor passages when a rotor blade enters and leaves the non-admitted area respectively. The following two equations are used to determine the frequencies of excitation caused by stator wakes and part admitted channel.

$$f_{\text{stator}} = \Omega \cdot z_{\text{stator}} = 2 \cdot \pi \cdot N_{\text{T}} \cdot z_{\text{stator}}$$
$$f_{\text{partial}} = \Omega \cdot z_{\text{block}} = 2 \cdot \pi \cdot N_{\text{T}} \cdot z_{\text{block}}$$

Results of tangential forces from transient calculations at the full and partial admission case are depicted in figure 11. These forces are calculated for each circumferential position by integrating the pressure on a single blade surface with the post processing tool Ansys CFX-POST.

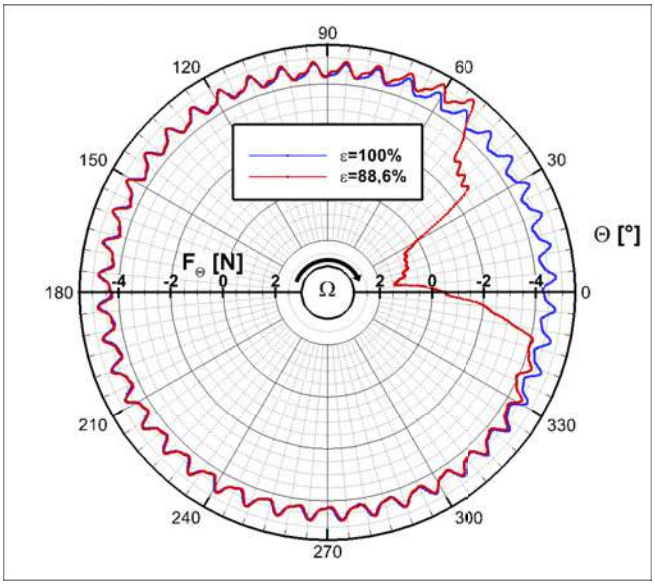

Figure 11. Tangential force at rotor blade for one revolution

As above mentioned, due to the same total (stage inlet) to static (stage outlet) pressure ratio amplitudes of forces in admitted arc of the partial admission case are comparable with forces of the full admission case. However, amplitudes of the forces which occur when rotor blades enter and leave the admitted arc increase significantly. Furthermore, a change of sign occurs by passing through the not admitted arc. When a rotor blade leaves the admitted arc first of all, the suction side of the blade enter the arc downstream of the blockage. On this side the passage can not be supplied by the working medium, so the static pressure decreases whereas the pressure side is still admitted. As a result, a raised tangential force in rotational direction can be observed whereby the amplitude is one order of magnitude higher compared to the amplitude of force caused by stator wakes. However, when the rotor leaves the blocked arc the suction side will be admitted with the working medium. Simultaneously, on the pressure side of the blade a pressure drop can be observed caused by the emptying of the rotor passage during passing of the blockage area. Due to the change of sign the tangential force the single blade counteracts the rotor wheel and acts as a compressor. Therefore, for each revolution the rotor blades are loaded alternating towards and opposite the rotational direction respectively. Figure 12 shows the frequency spectra of the tangential force.
Although, the excitation frequency due to part loading is considerably lower than the excitation caused by the stator wakes the amplitudes are obviously larger and dominate the frequency spectra. Additional frequencies caused by constructional components do not occur, however linear combination of the first both can affect on the frequency spectra. Further excitation frequencies occur in the frequency spectra but the two effects mentioned above dominate.

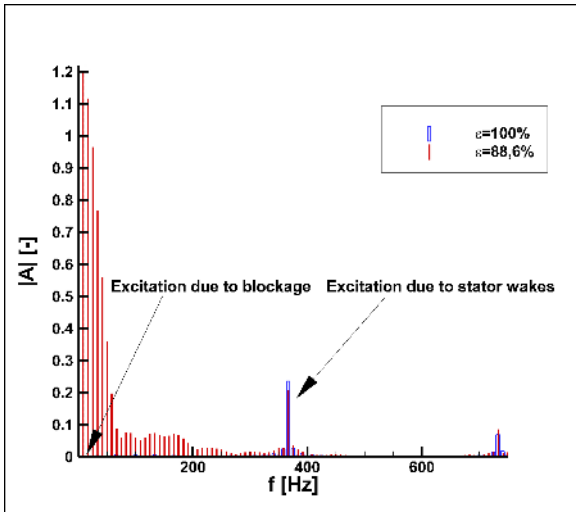

Figure 12. Frequency spectra of tangential force at rotor blade

Structural analysis
Figure 13 shows the results from the structural analysis and different engine orders caused by stator/rotor interaction as well as caused by the blockage (EO2=two borders of the blockage) and by 6 struts positioned in the inlet casing.

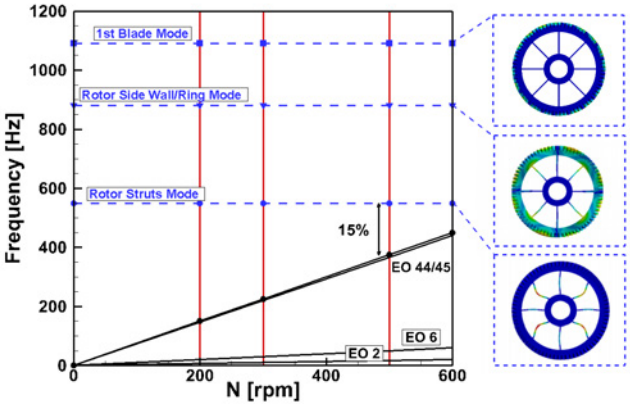

Figure 13. Campbell diagram of structural analysis of rotor

A noticeable shift between the first crossing point, where resonance can be expected and the intended operating point is recognizable, so that resonance problems in the system can be excluded. The first critical mode occurs at the frequency of approximatly $550Hz$ as the bending mode of the rotor struts. Another operating points including resonance can be leave out of consideration, because of a large shift to the design point.

Estimation of fluctuations:
Besides the safety aspect of the structural analysis, these investigation is necessary for consideration of forced response effects.
The positions of the piezoresistive transducers on the rotor

blades are specified based on the transient results of the simulations at full and partial admission. Therefore, local evaluation points at different positions at midspan of the rotor blade are defined in the numerical model. A total of 12 positions along the blade profile are evaluated for one revolution of the rotor blade. The figure 14 shows the corresponding results.

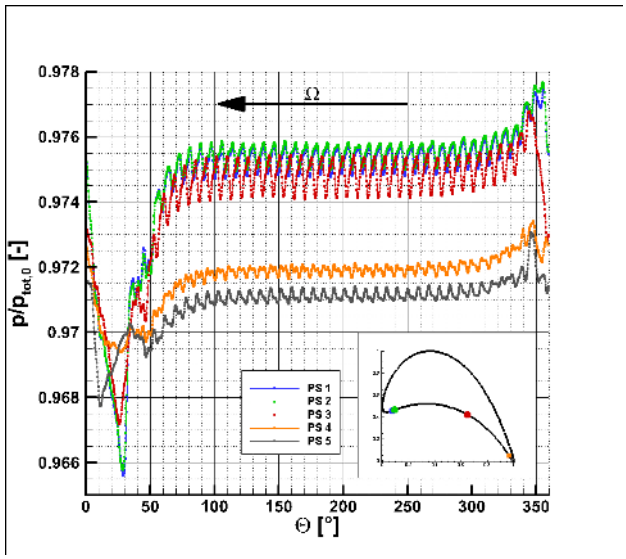

(a) Pressure side

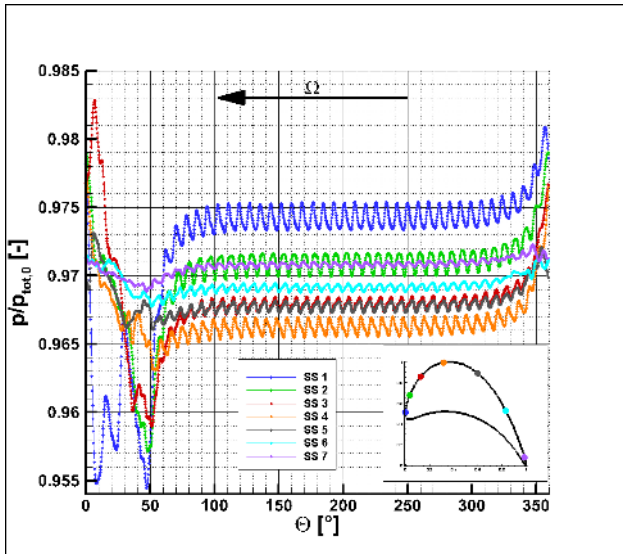

(b) Suction side

Figure 14. Static pressure at rotor blade for one revolution

A noticeably difference of the pressure level on suction and pressure side can be observed. Furthermore, the influence by the stator wakes are distinctly less compared to the disturbance due to the part admitted channel. Nevertheless, the amplitudes are not negligible and are neccessary to determine all excitations on the rotor blades. Two turning points in the graph of the transient behaviour of pressure occur while passing the blockage region, when the rotor entries and leaves the not admitted area respectively. First, at beginning of the blockage a minimum of the pressure is recognizable, whereas at the end of the blockage a maximum appears. Immediately, as the rotor blade enters the blockage, the emptying process of the rotor passage causes a reduced pressure. The interruption of the air supply downstream of the blockage causes the momentum of the remaining medium to decrease until the end of the blockage. When entering the admitted area, the high momentum flow impinges the rotor passage and will decelareted due to the low momentum flow in the passage. The stagnation of the fluid causes an increasing of the static pressure raising up to the maximum value. The emptying and filling process between the entering and leaving of the blockage is observable for each position of the rotor blade but with different intensity. Close to the rotor trailing edges the amplitudes of the pressure signal are one order of magnitude weaker than the amplitudes far from the traling edge or near to the leading edge repectively. The positions of the points DS 4 and 5 correspond to two points near to the traling edge and show the lowest response not only in the admitted but also in the not admitted area.
In figure 15 the frequency spectra of the pressure history is depicted and shows the predominant frequencies for pressure and suction side of the rotor blade.

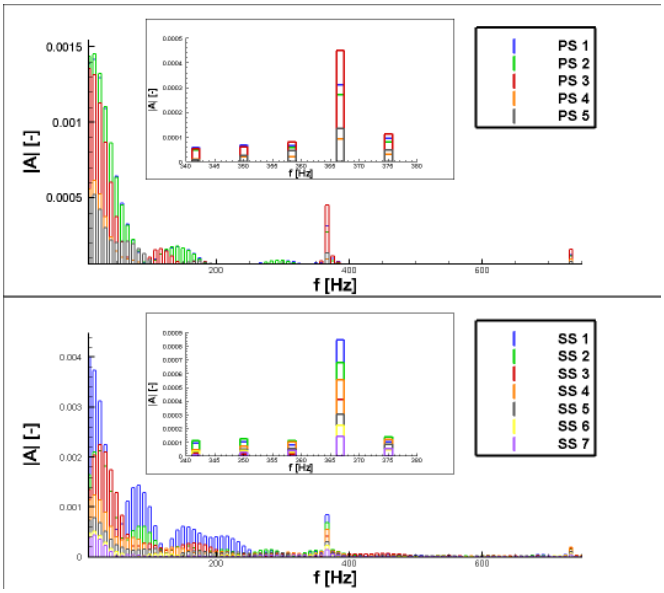

Figure 15. Rotor frequency spectra at different positions (top: pressure side=PS, bottom: suction side=SS

On pressure and suction side the low frequency excitation due to the blockage causes the highest amplitudes, whereby the magnitude of the amplitudes on the suction side are generally higher. In addition, the high frequency disturbance caused by the stator wakes are clearly recognizble at the frequency of $f = 366.66Hz$ as well as the multiple magnitude at $f = 733.33Hz$. Even higher frequencies are not noticeable, so the maximum sampling rate of 50kHz per channel performed by the A-D converter is sufficient for the proposed investigations.

5. CONCLUSION

In this paper the redesign of an existing low pressure test facility to a single stage facility for investigations to partial admission effects is described. In the first step, a suitable stage with characterstics of a control stage at design point was designed successful. The degree of reaction as well as the stage loading are comparable to corresponding values of a control stage in actual steam turbines. In doing so, the dominating effects of partial admitted stages can be measured even though the flow conditions in the test facility are not comparable to conditions of a control stages in steam turbines. After determination of a stage with characteristics of a control stage, numerical investigation with CFD and FEM methods were carried out. The CFD calculations have included steady state and transient simulations under full and partial admission conditions. Based on these results fields of influence and importance for the later following experimental investigations are determined. Furthermore, excitation sources caused by the unsteady flow are determined and compared with eigenfrequencies of the rotor wheel in a Campbell diagram. This indicates that neither at the design point nor at other proposed operating points the frequencies of excitation corresponds with any eigenfrequency. Thus, an operating point under resonance conditions can be excluded for all operating points which have to been investigated.

In addition, to specify the characteristics of the measurement technique fluctuations of the velocity and pressure field were estimated. Therefore, the frequency spectra was evaluated for different positions in the flow field and dominant frequencies and amplitudes could be identified and at once the positions where the measurment has to been placed. Based on the flow conditions in the test facility highly sensitive measurement is demand to resolve the fluctuations and to ensure small measurement errors.

In addition to the successfull design process of the test facility, the results shows the importance of the investigations of partial admission effects in the design process of control stages once more. The intended measurement at the retrofitted test facility as well as the corresponding numerical investigations have to give a wide indication of the unsteady flow in a part admitted control stage. Redesign of the low pressure test facility to a control stage enables extensive experimental investigations of partial admission effects in the future. An incomparable spatial as well as temporal resolution of a partly admitted control stage will ensure high quality data for further numerical validation and increase the comprehension of the phenomena, which occur at partial admission.

NOMENCLATURE

$\dot{m}$ $[\frac{kg}{s}]$ Massflow

ϵ $[-]$ Degree of admission

Ω $[\frac{1}{s}]$ Angular velocity

Ψ $[-]$ Stage loading

ρ $[\frac{kg}{m^3}]$ Density

ρ_y $[-]$ Degree of reaction

Θ $[deg]$ Circumferential position

F_Θ $[N]$ Tangential Force

l_{ax} $[m]$ Axial distance

c $[\frac{m}{s}]$ Velocity

c_p $[-]$ Pressure coefficient

f $[\frac{1}{s}]$ Frequency

Ma $[-]$ Mach number

n $[\frac{rev}{s}]$ Rotational speed

p $[Pa]$ Static pressure

P $[W]$ Power of blower

Re $[-]$ Reynolds number

w $[\frac{m}{s}]$ Velocity in relative frame

z $[-]$ Blade number

REFERENCES

[1] Aulich, A.-L. ; Sauer, T. ; Iseni, S. ; Moreau, A. ; Peitsch, D. ; Mailach, R. ; Micallef, D. ; Enghardt, L. ; Nicke, E. : Fan casing contouring under consideration of aeroacoustics, mechanics, aeroelasticity and whole engine performance. In: *Deutscher Luft- und Raumfahrtkongress 2015*, 2015

[2] Bohn, F. ; Funke, H.-H.-W. : Experimental Investigations Into the Nonuniform Flow in a 4-Stage Turbine With Special Focus on the Flow Equalization in the First Turbine Stage. In: *Proceedings of ASME Turbo Expo 2003* Volume 6 (Atlanta, Georgia, USA, June 16-19, 2003)

[3] Drexler, C. : *Strömungsvorgänge und Verlustanteile in ungleichförmig beaufschlagten Turbinenstufen*, RWTH Aachen, doctoral thesis, 1996

[4] Fridh, J. : *Experimental Investigation of Performance, Flow Interactions and Rotor Forcing in Axial Partial Admission Turbines*, KTH, School of Industrial Engineering and Management (ITM), Energy Technology, Heat and Power Technology, doctoral thesis, 2012

[5] Gao, K.-K. ; Wang, S.-S. ; Shi, D.-B. : Unsteady flow and load in 50% partial admission control stage with different admitting arc distributions. In: *Thermal Science* 20 (2016), Nr. suppl. 3, S. 805–813. `http://dx.doi.org/10.2298/tsci160201203g`. – DOI 10.2298/tsci160201203g

[6] He, L. : Computation of unsteady flow through steam turbine blade rows at partial admission. In: *Proceedings of the Institution of Mechanical Engineers, Part A: Journal of Power and Energy* 211 (1997), Nr. 3, S. 197–205. http://dx.doi.org/10.1243/0957650971537105. – DOI 10.1243/0957650971537105

[7] Hushmandi, N. B.: *Numerical Analysis of Partial Admission in Axial Turbines*, KTH Stockholm, doctoral thesis, 2010

[8] Iseni, S. ; Micallef, D. ; Mailach, R. : Investigation of Inlet Distortion on the Flutter Stability of a Highly Loaded Transonic Fan Rotor. In: *ASME Turbo Expo 2016: Turbomachinery Technical Conference and Exposition Volume 7B: Structures and Dynamics* (Seoul, South Korea, June 13–17, 2016), Nr. ASME Paper No. GT2016-56593

[9] Kalkkuhl, T. J.: *Strömungssimulation einer teilbeaufschlagten Dampfturbine*, Ruhr-Universität Bochum, doctoral thesis, 2014

[10] Lampart, P. ; Szymaniak, M. ; Kwidzinski, R. : Numerical Investigation of Unsteady Flow in a Partial Admission Control Stage of a 200MW turbine. In: *Proc. 6thEuropean Conference on Turbomachinery Fluid Dynamics and Thermodynamics* (Lille, France, March, 2005)

[11] Mutlu, E. : *Numerische Untersuchung zur Teilbeaufschlagung innerhalb einer Niedergeschwindigkeitsforschungsturbine bei 30°, 40° und 60° Versperrung*, Ruhr-Universität Bochum, master thesis, 2016

[12] Sinkwitz, M. ; Engelmann, D. ; Mailach, R. : Experimental Investigation of Periodically Unsteady Wake Impact on the Secondary Flow in a 1.5 Stage Full Annular LPT Cascade with Modified T106 Blading. In: *Proceedings of ASME Turbo Expo 2017* (Charlotte, NC, USA, June 26-30, 2017), Nr. ASME Paper No. GT2017-64390

[13] Tajc, L. ; Bednar, L. ; Polansky, J. ; Stastny, M. : Radial Control Stage with Partial Steam Admission. In: *Proceedings of the 8 th International Symposium on Experimental and Computational Aerothermodynamics of Internal Flows* (Lyon, France, July, 2007), Nr. Paper No. ISAIF8-0014

[14] Tokuyama, Y. ; Funazaki, K. ichi ; Kato, H. ; Shimiya, N. ; Shimagaki, M. ; Uchiumi, M. : Computational Analysis of Unsteady Flow in a Partial Admission Supersonic Turbine Stage. In: *ASME Turbo Expo 2014* Volume 2D: Turbomachinery (Düsseldorf, Germany, June, 2014), Nr. ASME Paper No.GT2014-26071. http://dx.doi.org/doi:10.1115/GT2014-26071. – DOI doi: 10.1115/GT2014–26071

[15] Walzer, P. : *Teilbeaufschlagung von Dampfturbinenregelstufen*, RWTH Aachen, doctoral thesis, 1970